SPH ANALYSIS OF EXTREME WAVE DIRECTIONALITY ON THE DYNAMICS OF FLOATING OFFSHORE WIND TURBINES

Shengzhe Wang
Department of Civil Engineering
University of Colorado Denver
Denver, CO 80204, United States
shengzhe.2.wang@ucdenver.edu

Wei-Liang Chuang
Department of Marine Environment and Engineering
National Sun Yat-sen University
Kaohsiung 80424, Taiwan
wlchuang@mail.nsysu.edu.tw

I. INTRODUCTION

Harnessing renewable energy through floating offshore wind turbines (FOWT) represents a crucial step towards the decarbonization of the world's energy infrastructure for climate change adaptation. However, their susceptibility to severe sea conditions (including extreme and breaking waves) may result in damage or a degradation in power generation efficiency. It is therefore necessary to explore their complex dynamic behavior under extreme hydrodynamic events to ascertain the feasibility of potential FOWT designs across diverse sea states.

At present, the most common approach for the hydrodynamic analysis of FOWTs utilizes potential theory (e.g., via ANSYS/AQWA or FAST), also referred to as "mid-fidelity" solutions [1]. Such solvers present a computationally efficient method to describe fluid flows by deriving the velocity potential function based on the Laplace equation. Despite their popularity, mid-fidelity solvers exhibit several limitations. Since potential-flow theory is inherently inviscid, Morison's equation is commonly applied to introduce drag forces via a quadratic damping model where its coefficients are reliant upon experimental data. Potential theory also cannot address turbulence effects and suffer difficulties when attempting to model highly nonlinear flow regimes induced by extreme or breaking waves.

Since FOWTs are commonly exposed to harsh ocean environments, the use of "high-fidelity" computational fluid dynamics (CFD) is necessary for load prediction under extreme conditions. Currently, the majority of CFD methods employ Eulerian mesh-based techniques (e.g., finite volume method in OpenFOAM) to solve the Navier–Stokes equations governing fluid dynamics. Advancements in computational hardware (e.g., GPUs) have also increased the popularity of Lagrangian mesh-free techniques such as Smoothed Particle Hydrodynamics (SPH) within coastal and offshore engineering [2]. SPH exhibits the advantage of not requiring special treatment for large density discontinuities (e.g., at the free surface), nor suffer mesh distortion during large deformation or discontinuous flow (e.g., wave breaking). While SPH has been successfully used to model floating structures under regular or irregular waves [3,4], the method has only seen limited validation against breaking waves [5] and has seldomly been applied for such applications. The complexity in the modelling of such phenomena (both experimental and numerical) has further contributed to a severe deficit in the analysis of FOWTs subjected to breaking waves.

This work first validates weakly compressible SPH against experimental observations of a plunging breaker impacting a moored floating structure. The method is next employed to examine the hydrodynamics of a semi-submersible FOWT subjected to nonbreaking and breaking waves approaching from three different directions. The objective is to quantify extreme wave forces, mooring loads, and structural accelerations as a function of wave directionality and impact characteristics for the first time. Through this process, we reveal the importance and implications of breaking wave impingement on FOWTs to improve their resilience in harsh marine climates, affirming the role of SPH in supporting engineering design in this field.

II. SPH MODELING AND VALIDATION

This research employs the CUDA-accelerated open-source SPH solver DualSPHysics v5.2 [2] for the simulation of floating body dynamics. The discretized momentum equation governing the motion of fluid particles was described via an artificial viscosity model (with $\alpha = 0.01$) adopting the Wendland quintic kernel. Weakly compressible conditions were assumed with the pressure-density relationship given by Tait's equation of state [2]. For solid surfaces, dynamic boundary conditions (DBC) were adopted where boundary particles exhibit the same continuity and state equations as their fluid counterparts. Floating objects are assumed to behave like rigid bodies with linear and angular velocity determined via their governing equations of motion [4]. MoorDyn [6] was adopted for the treatment of mooring forces by discretizing a mooring line into point masses connected using linear spring–damper segments. When MoorDyn is coupled with DualSPHysics, the motion of floating bodies is used as input to update the position of mooring lines and the determination of mooring forces at the fairleads. Such forces are then imposed as external loads onto the floating

model which updates the position of the floater (repeated at each timestep). Time-stepping was conducted via the Verlet scheme according to the Courant–Friedrichs–Lewy (CFL) condition [2].

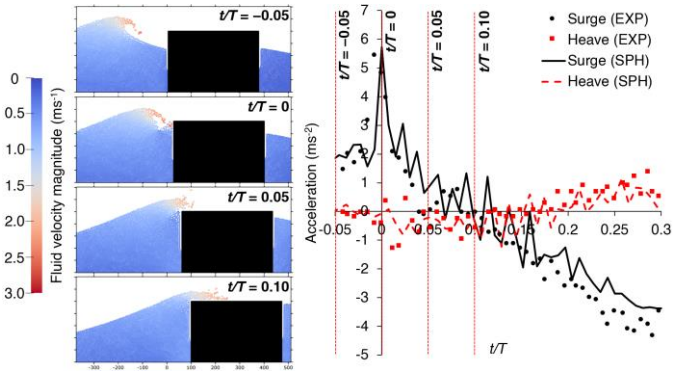

Figure 1. Evolution of SPH wave profile and TLP accelerations in surge and heave compared between the experiment (EXP) and SPH

DualSPHysics was benchmarked against a breaking wave impingement experiment performed by Chuang et al. [7]. The setup consisted of a Plexiglass box 0.37 m long, 0.31 m high, and 0.85 m wide placed within a 36 m long and 0.9 m wide flume, imitating a tension-leg platform (TLP). The TLP had a total mass of 17.0 kg and was placed within water 0.80 m deep with a draft of 0.20 m. Four 1.6 mm wire tendons were used to anchor each corner of the structure to the flume bed. A plunging breaking wave with height H = 0.17 m and period T = 1.32 s was generated via wave focusing which impinged upon the forward face of the TLP (Fig. 1). The motion of the box during impact was captured using a high-speed camera recording at 1000 frames per second.

The TLP and its moorings were replicated via SPH and Moordyn, respectively, where the breaking wave was generated using extreme wave focusing through a piston wavemaker with its stroke (x_p) given by:

$$x_p(t) = \sum_{i=1}^{N} \frac{A_i}{\chi_i} \cos\left[-k_i x_f - \omega_i (t - t_f)\right] \quad (1)$$

with ω_i, k_i, and A_i respectively denoting the frequency, wavenumber, and amplitude of the i^{th} wave component, across N = 100 total components taken from an underlying JONSWAP spectrum adopting a significant wave height H_s = 0.29 m and peak period T_p = 1.32 s. χ_i is the Biesel transfer function to convert A_i into an equivalent linear stroke, while x_f and t_f respectively are the theoretical focused wave location (relative to the wavemaker) and time when the extreme wave is desired.

The TLP maximum surge and heave computed using SPH were first examined across initial interparticle spacing (Δp) distances between 10 and 1.25 mm to reveal the particle resolution required to achieve convergence of the numerical response. Based on the convergence study, Δp = 5.0 mm was adopted, giving $H/\Delta p$ = 44. This finding is consistent with existing literature which recommend $H/\Delta p$ ratios in the range of 36 to 40 for the simulation of breaking waves using SPH [8]. Likewise, a CFL coefficient of 0.2 was observed to be sufficient for temporal convergence.

After ensuring spatial and temporal convergence, the experimental and numerical surge and heave acceleration of the TLP were compared in Fig. 1. It is seen that both components were well predicted by DualSPHysics–Moordyn. However, SPH was unable to capture water-air mixing between the wave front and TLP as well as fluid ejecta produced by the impact. To account for such effects would necessitate the use of 3D multi-phase (liquid–gas) models at a much finer resolution which may prove computationally prohibitive [9].

III. Analysis of Extreme Wave Impact on FOWT

A. FOWT Description and Modeling

The 5-MW semi-submersible OC5-DeepCwind turbine developed by the National Renewable Energy Laboratory (NREL) [10] was adopted to investigate breaking wave impact on FOWTs. The substructure comprises three 12-m diameter pontoons each atop a 24-m diameter heave plate. Each pontoon sits at the vertex of an equilateral triangle with sides 50 m and are linked to the 6.5-m diameter tower via a network of 1.60-m diameter cross braces. The FOWT is situated in water 200 m deep and exhibits a total draft of 20 m. Three 836-m catenary mooring lines (labeled L1, L2, and L3 in Fig. 2a) spaced 120° apart are used to anchor the structure to the seabed giving a mooring radius of 837.6 m when taken from the tower axis (Fig. 2a). The turbine nacelle is located 90 m above the still water level (SWL) whereas the FOWT's center of gravity (COG) is 8.07 below the SWL. A detailed description of the structural and mooring properties can be found in Robertson et al. [10].

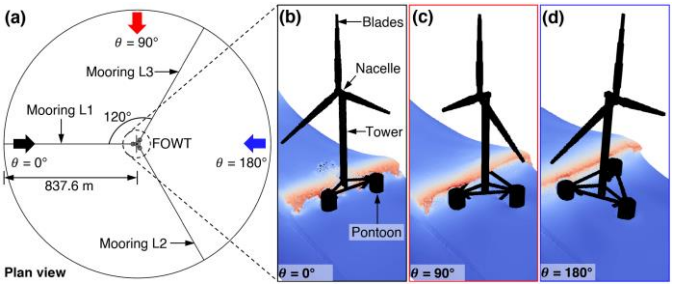

Figure 2. (a) Plan view of OC5-DeepCwind FOWT showing breaking wave approaching from (b) 0°, (c) 90°, and (d) 180°

The FOWT's geometry was first created in SketchUp Pro then imported into DualSPHysics. The fluid domain has a total length, width, and depth of 770 m, 120 m, and 80 m, respectively, and was localized around the FOWT to reduce computational cost without compromise to the flow field's fidelity. Consequently, most of the mooring lines lie beyond fluid coverage but this does not influence the transfer of information between DualSPHysics and the MoorDyn solver [3]. A JONSWAP spectrum (H_s = 29 m and T_p = 13.2 s) was adopted to generate a focused breaking wave, as per Eq. 1, with wave height H = 27 m (T = 10.9 s) as consistent with the largest waves observed during Hurricane Ivan in 2004 [11]. For comparison, a nonbreaking extreme wave with the same H (but with T = 11.5 s) was also generated using a different frequency spectrum. The FOWT's tower was positioned at a distance of 320 m from the wavemaker as this resulted in the largest impact forces being produced by the plunging breaker. To simulate

waves approaching from different directions, the FOWT and its moorings were orientated at $\theta = 0°$, 90°, and 180° relative to the domain's longitudinal axis, as shown in Fig. 2b, c, and d, respectively. For this study, $\Delta p = 0.75$ m was adopted resulting in $H_b/\Delta p = 36$ and a total particle count exceeding 14.3 million. A total physical time of 130 s was simulated which took approximately 17 hours on an NVIDIA RTX 3090 GPU.

B. SPH Results

The total horizontal wave force (F_x) as a function of wave direction (θ) is summarized in Fig. 3a which includes both breaking and nonbreaking waves. Despite their identical wave heights of $H = 27$ m, the force maximum resulting from breaking wave impingement on the FOWT is greater than their nonbreaking counterparts across all considered wave directions. In addition, the largest force was observed for $\theta = 0°$ with a 70% increase in F_x induced by wave breaking. However, $\theta = 180°$ yielded the highest nonbreaking wave force on the pontoons.

The structural accelerations generated by breaking and nonbreaking waves on the FOWT were next compared (Fig. 3b). Given its rigid body response, the accelerations at the nacelle (a_n) can be determined via the superposition of the surge (a_x) and pitch ($a_{\theta y}$) acceleration time history taken about the COG per:

$$a_n(t) = a_x(t) + GN \times a_{\theta y}(t) \quad (2)$$

where $GN = 98.07$ m denotes the vertical distance from the COG to the nacelle. For $\theta = 0°$, the peak nacelle acceleration of 6.93 ms^{-2} (0.71g) produced from wave breaking is seen to be approximately 230% larger than that from its nonbreaking counterpart (2.10 ms^{-2}). Likewise, breaking waves approaching from $\theta = 180°$ resulted in an 86% increase in a_n relative to its nonbreaking counterpart. These results could have significant implications towards the structural design of turbine towers due to the dynamic amplification of lateral forces. However, maximum nacelle accelerations for $\theta = 90°$ were largely comparable between breaking and nonbreaking impact.

Fig. 3c summarizes the maximum mooring tensions (F_T) at the fairlead for breaking and nonbreaking waves. Note that the mooring line (L1, L2, or L3 – see Fig. 2a) experiencing F_T for a given θ is also labeled in Fig. 3c. Contrary to F_x and a_n, maximum tensions across the three moorings were produced by the nonbreaking extreme wave across all θ. This observation is likely explained by its longer loading duration, which contrasts with the relatively short impact produced by wave breaking.

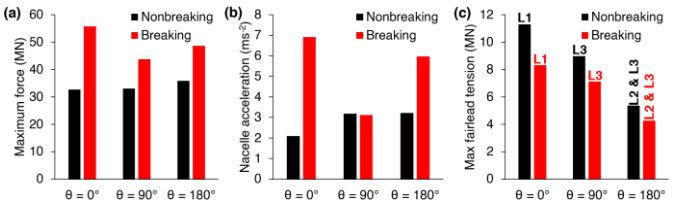

Figure 3. (a) Maximum force, (b) nacelle acceleration, and (c) fairlead tension for nonbreaking/breaking waves approaching from direction θ

IV. Conclusions

This paper successfully validates SPH for the prediction of a plunging breaker impacting a model TLP against physical experiments. Next, SPH was adopted to simulate the hydrodynamic response of the NREL semi-submersible OC5-DeepCwind subjected to both breaking and nonbreaking extreme waves (with the same wave height) consistent with Hurricane Ivan approaching from three different directions relative to the FOWT. The major conclusions are as follows:

- An $H/\Delta p$ of 44 was sufficient to achieve spatial convergence when modeling breaking waves impacting a moored floating structure in 2D.
- The largest forces and nacelle accelerations were generally produced by breaking waves across all considered directions. Notably, $\theta = 0°$ yielded the greatest F_x and a_n.
- For all θ, nonbreaking waves imparted higher mooring tensions due to their longer loading duration, with $\theta = 0°$ witnessing the largest F_T on L1.

Ultimately, this research provides novel insight into the role of extreme waves on the dynamics of FOWTs. In doing so, we foster increased awareness on the necessity of considering impulsive wave impact approaching from multiple directions to improve their survivability in harsh marine environments, proving SPH conducive to achieving engineering-relevant prediction for offshore renewable energy systems.

Acknowledgement

This research was partially supported by the Office of Research Services at the University of Colorado Denver and the National Science and Technology Council of Taiwan under grant NSTC 112-2636-E-110-007.

References

[1] Zeng X, Shao Y, Feng X, Xu K, Jin R, Li H. Nonlinear hydrodynamics of floating offshore wind turbines: A review. Renewable and Sustainable Energy Reviews 2024;191.
[2] Dominguez JM, Fourtakas G, Altomare C, Canelas RB, Tafuni A, Garcia-Feal O, et al. DualSPHysics: from fluid dynamics to multiphysics problems. Computational Particle Mechanics 2022;9:867–95.
[3] Tan Z, Sun P, Liu N, Li Z, Lyu H, Zhu R. SPH simulation and experimental validation of the dynamic response of floating offshore wind turbines in waves. Renewable Energy 2023;205:393–409.
[4] Wang S. Analytical solutions for the dynamic analysis of a modular floating structure for urban expansion. Ocean Engineering 2022;266.
[5] Salis N, Hu X, Luo M, Reali A, Manenti S. 3D SPH analysis of focused waves interacting with a floating structure. Applied Ocean Research 2024;144:103885.
[6] Hall M. MoorDyn - Users Guide 2015.
[7] Chuang W, Chang K, Mercier R. Green water velocity due to breaking wave impingement on a tension leg platform. Experiments in Fluids 2015;56.
[8] Didier E, Neves DRCB, Martins R, Neves MG. Wave interaction with a vertical wall: SPH numerical and experimental modeling. Ocean Engineering 2014;88:330–41.
[9] Pawitan KA, Garlock M, Wang S. Multiphase SPH Analysis of a Breaking Wave Impact on Elevated Structures with Vertical and Inclined Walls. Applied Ocean Research 2024;142.
[10] Robertson AN, Wendt F, Jonkman JM, Popko W, Dagher H, Geuydon S, et al. OC5 project phase II: Validation of global loads of the DeepCwind floating semisubmersible wind turbine. Energy Procedia 2017;137:38–57.
[11] Wang DW, Mitchell DA, Teague WJ, Jarosz E, Hulbert MS. Extreme waves under Hurricane Ivan. Science 2005;309:896.